CONF-9004136--9-Rev.

UCRL--101932-Rev.1

DE90 016211

AUG 3 1 1990

RAILGUN PERFORMANCE WITH A TWO-STAGE LIGHT-GAS GUN INJECTOR

R. S. HAWKE
et. al.

5th Symposium on
Electromagnetic Launch Technology
Destin, FL

April 2-5, 1990

Lawrence Livermore National Laboratory

RAILGUN PERFORMANCE WITH A TWO-STAGE LIGHT-GAS GUN INJECTOR*†

R. S. Hawke and A. R. Susoeff, Lawrence Livermore National Laboratory, Livermore, CA

J. R. Asay, J. A. Ang, C. A. Hall, C. H. Konrad and G. W. Wellman
Sandia National Laboratories, Albuquerque, NM

R. J. Hickman, W. A. Heath and J. R. Martinez, Ktech Corporation, Albuquerque, NM

J. L. Sauve' and A. R. Vasey, EG&G, Albuquerque, NM

M. Shahinpoor
University of New Mexico, Albuquerque, NM

ABSTRACT
This paper summarizes the results obtained with the HELEOS railgun which uses a two-stage light-gas gun (2SLGG) as an injector [1]. The high velocity 2SLGG injector pre-accelerates projectiles up to ~7 km/s. The high injection velocity reduces the exposure duration of the railgun barrel to the passing high temperature plasma armature, thereby reducing the ablation and subsequent armature growth. The 2SLGG also provides a column of cool, high pressure hydrogen gas to insulate the rails behind the projectile, thereby eliminating restrike. A means to form an armature behind the injected projectile has been developed. In preliminary tests, the third stage railgun has successfully increased the projectile velocity by 1.35 km/s. Extensive diagnostics have been used to determine the behavior of the armature and track the launcher's performance. In some cases, velocity increases in the railgun section have been achieved, which are in close agreement with theoretical predictions, whereas in other experiments deviations from theoretical have been observed. The reasons for and implications of these results are addressed. Recent tests are reported.

INTRODUCTION
STARFIRE is a joint Sandia National Laboratories, Albuquerque/Lawrence Livermore National Laboratory (SNLA/LLNL) program based at SNLA that has as its goal the development of a hypervelocity launcher for use as a high-pressure research tool [1, 2]. The launcher combines a two-stage light-gas gun (2SLGG) with a railgun. The 2SLGG is used as a projectile pre-accelerator/injector [1, 3], to the railgun. The launcher is designated HELEOS - Hypervelocity Experimental Launcher for Equation Of State.

The STARFIRE system uses the 2SLGG to minimize barrel ablation and armature contamination. Hydrogen is used as the propulsive injection gas which provides injection velocities of 5 to 7 km/s and a nearly pure hydrogen environment immediately behind the projectile as it enters the railgun barrel. The hydrogen gas also serves to insulate the rails and thereby reduce the probability of forming secondary arcs.

REQUIREMENTS FOR SUCCESSFUL OPERATION
In order to successfully employ a 2SLGG as a hypervelocity injector followed by electromagnetic acceleration of a projectile, several challenges had to be met. The challenges included: 1) refinement of the use of a 2SLGG in order to ensure the integrity of the projectiles; 2) development of the projectile sealing capability in order to minimize blowby; 3) elimination of pre-arcs in front of the projectile; and 4) development of a reliable means of forming a propulsive armature upon entrance into the railgun section. During the past two years, all of these challenges have been met and more than 15 significant tests with successful armature formation, most with significant electromagnetic velocity increases, have been performed.

DESCRIPTION OF THE PROJECTILE DESIGN
The most challenging task was the development of a means to reliably form a propulsive armature upon injection of the projectile into the railgun section. In the course of acceleration in the 2SLGG, a boundary layer between the projectile and barrel forms [4, 5]. This boundary layer is warm but not hot enough to be sufficiently conductive to commutate current. The boundary layer is relatively cool and non-conductive and tends to insulate any metal fuse or armature forming element on the backside of the projectile, thus inhibiting the most common means by which lower velocity injected projectile armatures are formed. We tested several methods of armature formation including spark discharge [6], barrel mounted metal fuse vapor injection [7] and the technique now in use, a seeded boundary layer commutation through a projectile mounted metallic armature. Fig. 1 is a lengthwise sectional view of the projectile design (see figure caption for functional details). This design has proven to be very reliable at commutating a rail-to-rail current flow after 2SLGG injection into the railgun section. A full band of conductive seeding material was used up through H62. The full band had a tendency to conduct current, vaporize and form an undesirable confined armature. From Test H63 onward only partial rings were used with good success.

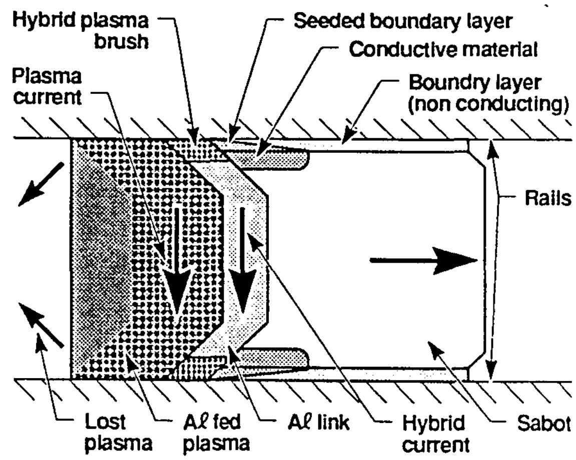

Fig. 1. Lengthwise section of projectile design illustrates the use of a thick A1 disc attached to the back side of the plastic sabot to serve as the metal link of a hybrid armature [8]. Conductive material is used to seed the boundary layer as it is eroded along with the sabot by the boundary layer. The seeding enables hybrid commutation at a few hundred volts. The Al armature first serves as the link for a hybrid armature. After a time, the ablated Al feed the region behind the Al armature and as plasma conduction begins, evolves into a tandem (hybrid/plasma) armature. The plasma tends to stay in close proximity to the hybrid and contributes to the propulsion of the projectile.

*Work performed under the auspices of the U. S. Department of Energy by Lawrence Livermore National Laboratory under contract W-7405-ENG-48 and Sandia National Laboratories under contract DE-AC04-76DP00789.

†This Paper was prepared for presentation at the 5th Symposium on Electromagnetic Launch Technology to be held April 2-5, 1990 at Destin, FL.

MODES OF ARMATURE FUNCTION OBSERVED

The projectile shown in Fig. 1 has been observed to function in four modes: 1) hybrid with current passing through two short plasma brushes between the metal link and rails; 2) "pure" plasma serving as the sole current path; 3) tandem where a hybrid is closely followed by a plasma and both provide propulsion; and 4) confined where current passes through the seeding band. The latter is not a desired mode and has been eliminated.

Fig. 2 is a muzzle voltage record which illustrates commutation and all four of the armature modes. The magnitude and duration of the initial commutation pulse indicates the difficulty of commutating current through the boundary layer (better seeding results in lower commutation voltage and shorter duration). A commutation voltage of ~900 V is shown in Fig. 2 while more recent tests have typically commutated at about 200 V. The subsequent high muzzle voltage indicates operation in a confined plasma mode [9]. The voltage drop to about 150 V indicates operation in the hybrid mode [8]. The ramp up to ~240 V is attributed to the rising plasma brush voltages associated with the increasing gap between the solid link and rails resulting from the erosion of the metal link and/or the recession of the rails away from the metal link. The recession is the result of pre-existing erosion of the rails from prior tests. When the voltage reaches ~240 V, it is clamped by a plasma armature which forms behind the hybrid. Gradually the plasma voltage decreases to about 200 V and dominates until projectile launch.

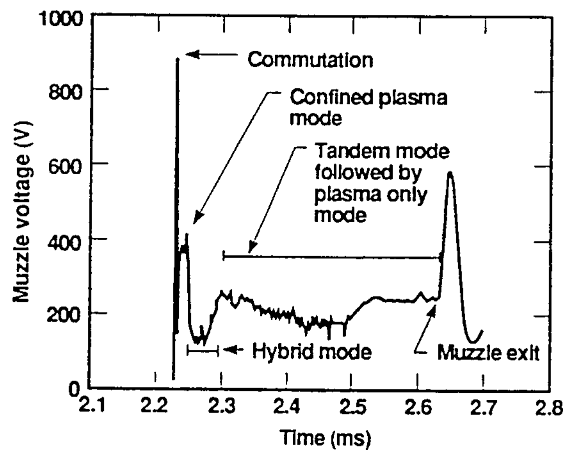

Fig. 2. Muzzle voltage vs. time record indicates mode of armature functioning. The first spike is associated with the rapid rise of the switched rail voltage until commutation between the rails occurs. In this case, a confined plasma is the first armature mode to occur. This mode results in a high armature voltage (~400 v) and is followed by the formation of a hybrid mode at a lower voltage (~170 v). The hybrid voltage ramps up as the plasma brush gaps become larger due to contact erosion and/or entrance into regions of the rails which are already eroded by previous tests. When the hybrid gaps are large enough to result in voltages exceeding a stable plasma voltage (~250 v), the armature transitions into a tandem mode and possibly a pure plasma mode prior to launch.

ARMATURE PERFORMANCE RATIO

A useful (and important) method of comparing the results of tests with different injection velocities, armature types and armature modes is to calculate the ratio, ξ, of the measured electromagnetic velocity increase Δv to the maximum theoretical velocity increase:

$$\xi = \frac{2 m_p \Delta v}{L' \int I^2 dt} \qquad \text{(Eq. 1)}$$

where L' is the launcher inductance gradient, I is the current input to the railgun and m_p is the projectile mass. An ideal performance ratio (ξ = 100%) would indicate the full propulsion of all the current input to the railgun and a complete lack of parasitic losses such as: 1) viscous drag acting on the projectile and/or plasma(s); and 2) kinetic drag "m-dot" from erosion or ablation of the barrel by the projectile or plasmas and/or released surface layers by a bow shock traveling in front of the projectile. A loss of performance would also accompany a current diversion from the propulsive armature by a pre-arc in front of the projectile, restrike behind the armature, and/or a splitting of some or all of the current away from the rear of the propulsive plasma. In our tests, we have effectively eliminated pre-arc and restrike. A lack of restrike might be the result of the hydrogen gas following the armature and/or the higher injection velocity. In all cases, the full current input level is reached immediately behind the projectile or at a point close behind. Some of our tests have indicated that all the current remained in close proximity of the projectile while others have indicated a separation or bifurcation of the armature into two or more regions.

TEST RESULTS

Table 1 is a numerical summary of 16 tests while Fig. 3 is a graphical representation of the results. Projectile mass ranged from 1.67g (H55) with a very thin A1 foil to serve as a plasma fuse to about 2.6g (H45, H49 and H65). Injection velocity ranged from 5.2 km/s (H49) to 6.56 km/s (H56). Launch velocity ranged from 5.47 km/s (H49) to 6.89 km/s (H78). Velocity increase by the railgun stage varied from 0 km/s (H48 and H55) to 1.35 km/s (H78). The overall performance ratio of each test varied from 0 to 75%. (Note: Although H40 and H45 indicate a large ξ, we believe some of the velocity again was the result of hydrodynamic boasts caused by: 1) rapid vaporization of the A1 armature during a fast rising current profile (H40) and 2) a rocket-like boost from a confined plasma (H45)[9]. Even though the confined mode provided a hydrodynamic velocity increase in H45, that was not

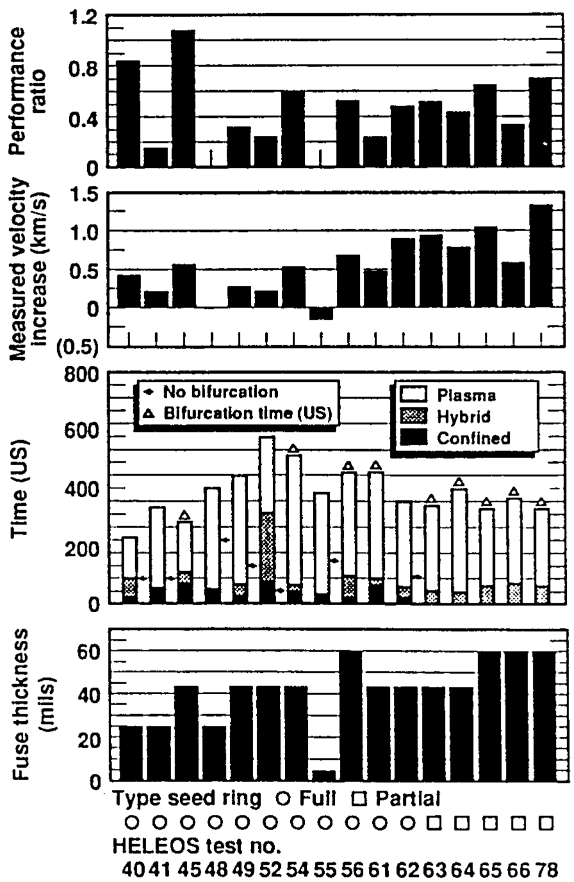

Fig. 3. Compilation of results from 16 tests. The bottom row indicates the test number; next row up the initial thickness of the Al armature. The third row is the approximate sequential time duration of each armature mode deduced from the muzzle voltage record. Bifurcation time, when it occurred and persisted, is indicated. The forth and fifth rows indicate the velocity gain and performance ratio respectively.

Table 1

Test No.	40	41	45	48	49	52	54	55	56	61	62	63	64	65	66	78
Projectile Mass (grams)	2.39	2.11	2.61	2.44	2.63	2.40	2.37	1.67	2.05	2.14	2.18	2.28	2.36	2.54	2.17	2.28
Armature Thickness (mm)	0.66	0.66	1.09	0.66	1.09	1.09	1.09	0.10	1.52	1.09	1.09	1.09	1.09	1.52	1.52	1.52
Injection Velocity (km/s)	5.67	5.44	5.73	5.63	5.2	5.84	5.46	6.27	6.56	5.96	5.92	5.81	5.75	5.37	6.1	5.54
Launch Velocity (km/s)	6.07	5.64	6.28	5.63	5.47	6.04	5.98	6.12	7.21	6.43	6.75	6.71	6.51	6.37	6.66	6.89
Velocity Increase (km/s)	0.4	0.2	0.55	0	0.27	0.2	0.52	-0.15	0.65	0.47	0.83	0.90	0.76	1.0	0.56	1.35
Performance Ratio (Percent)	95	17	108	0	33	24	58	0	53	24	48	52	44	65	34	75
Peak Current (kA)	223	220, 230*	260	230, 230*	220, 230*	320	315	290	340	430	427	410	423	408	395	435
Time To Peak Current (μs)†	93	77, 141*	89	105, 192*	90, 190*	94	84	122	109	112	102	90	98	110	100	95
Bifurcation Time (μs)†	100	112		205	110	60		112			118					
Commutation Voltage (V)	750	934	940	1100	580	1130	970	1160	416	888	895	438	250	235	227	1190

***Indicates peak current and time of peak current for second pulse from time sequenced capacitor bank modules.**
†Relative to start of current flow at commutation.

generally the case as seen in H41, H48, H52, H55 and H61. These two effects were eliminated from all other tests. Formation of a confined plasma was eliminated by changing the conductive material used for seeding the boundary layer from a complete rail-to-rail band to an incomplete band, beginning with H63.) Fig. 4 is a summary of the measured velocity increase vs. the theoretically possible electromagnetic velocity increase including estimated error bars for each test. Peak currents where 220kA to 435kA. A current of 435kA corresponds to a propulsion stress of 300 MPa (3.0 kb). The launcher is designed to operate up to 300 MPa and hasn't shown any signs of failure from any of the tests to date. In some cases (H41, H48 and H49) double current peaks were obtained by sequencing the discharge of additional capacitor modules. Armature bifurcation, when it occurred, was sometimes prior to peak current (H52), near peak current (H40 and H55) and significantly after first peak current (H41, H48, H49 and H62). Several tests indicated no distinguishable bifurcation occurred (H45, H54, H56, H61, H63-66 and H78).

Of all the tests reported above, H78 is the most useful to examine more closely because it represents a test in which relatively high performance was obtained. In this test, a velocity increase of 1.35 km/s (5.54 km/s to 6.89 km/s) was measured for a 2.3g projectile. This test also had the highest average performance that is completely electromagnetic (e.g. no significant electrothermal nor rocket velocity gain). Fig. 5A illustrates that the armature current rapidly rose to the total input current as the projectile passed the first and second B-dot positions and reached about 75% of total input at the third B-dot. The muzzle voltage indicates predominantly hybrid operation for about 60 μs (from 2400 μs to about 2460 μs) at which point the armature transitioned to a plasma.

Fig. 5B is a composite of the measured rail currents normalized by the total input current to the breech of the railgun. From this information, the time at which the armature current reached 20, 40, 60 and 80% of the input is found and used in Fig 5C along with the

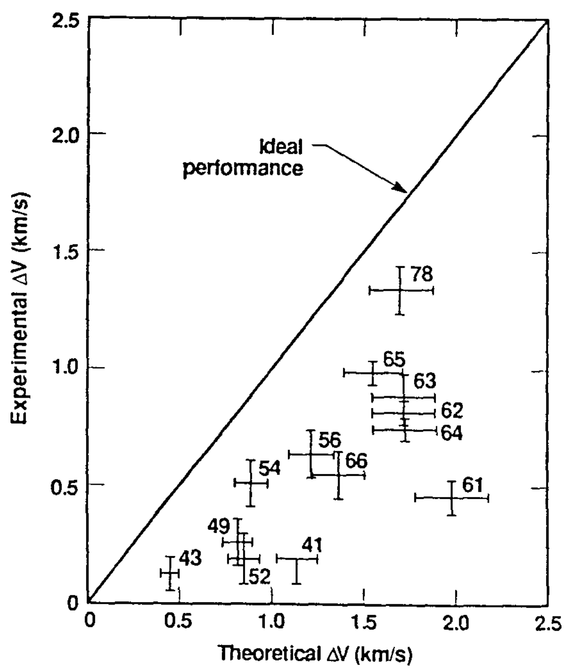

Fig. 4. Measured velocity increase vs. the theoretically possible electromagnetic velocity increase. The measured velocities are determined with fast pressure gauges and/or optical break beams at the input to the railgun and with flash X-Rays and/or MAVIS [10] velocity traps at the muzzle of the railgun. The measured input current is used to calculate the theoretical velocity gain.

projectile position. From this it can be seen that most of the current remained close to the projectile throughout the acceleration. Nearly all of the current was close until the projectile reached about 1.25 m (the position is in relation to a pressure gauge location) which is about 0.75 m into the railgun. Fig. 6A is a plot of the theoretical and measured projectile velocity increase vs. projectile position. The theoretical increase is based on all the input current serving to accelerate the projectile (per Eq. 1). In this case, the measured projectile velocity increase closely matched the theoretical up to about 1.2 km/s at about 1.4 m. At this point the acceleration began to diverge from the theoretical. The companion figure, 6B shows the estimated gap between the solid metal hybrid link and the rail surface vs. the projectile position. Initially the gap is small (~15 μm) but in the region between 1.4 m and 2.1 m the rails are significantly eroded by previous tests. The large gap results in less current flow through the plasma filled gap and hence the solid link, a reduction in the link vaporization rate and a reduction in supply of metallic ions to the front region of the plasma. Meanwhile, metallic ions are being lost from the rear portion of the plasma as a result of viscous friction between the plasma and the barrel [13]. When the replenishment rate drops below the loss rate, the plasma begins to lengthen as seen in the composite of the 20, 40, 60 and 80% current level contours most easily seen in Fig. 6B. There is most probably some growth in the link-rail gap resulting from the gradual erosion of the link. This erosion causes the muzzle voltage to increase (as seen in Fig. 5A) while the hybrid mode predominates (from 2400 μs to 2460 μs). In general, effective propulsion can be maintained so long as the current distribution can be kept close to the base of the projectile. In this case, that is achieved by plasma replenishment. While the replenishment is adequate, the plasma portion of the armature is effective. In most tests, it was found that the velocity increase exceeded the theoretical value that would have been obtained if only the current flow in the hybrid was taken into consideration. Hence we conclude that at least some of the velocity increase is from the plasma behind the hybrid, especially in H63, H64, H65, H66 and H78 where there was an absence of a confined armature (by design). Our hypothesis is that the plasma remains in contact with the projectile and propulsive, at least in part. This may be the result of plasma replenishment by the "gradual" vaporization of the Al armature. Tests to fully differentiate these effects are in progress.

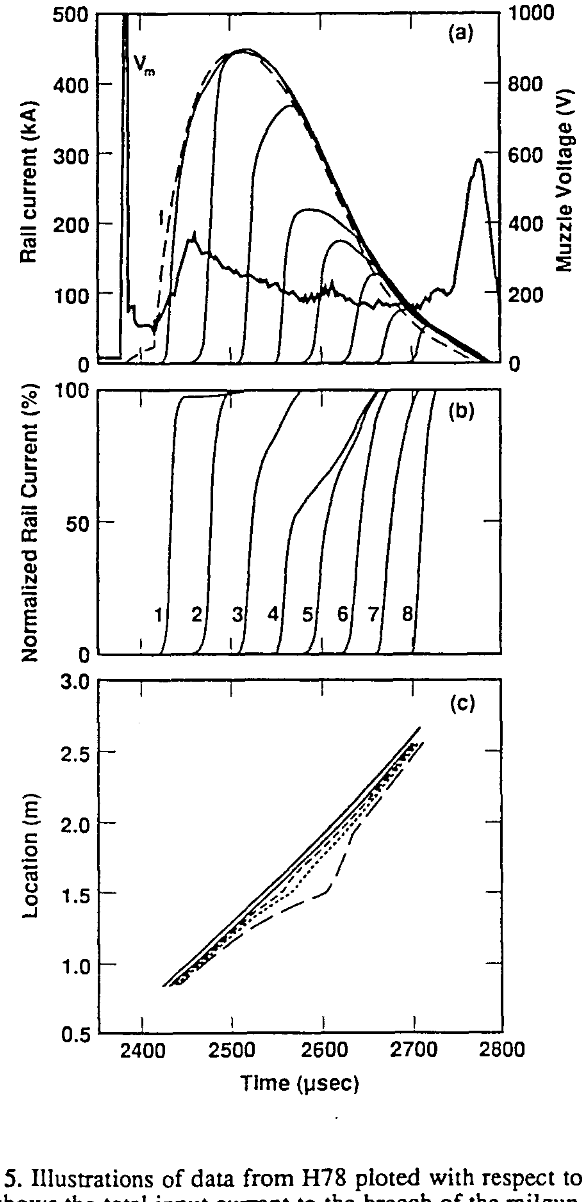

Fig. 5. Illustrations of data from H78 ploted with respect to time. 5A shows the total input current to the breech of the railgun along with eight of the integrated rail B-dot probes [11, 12]. The muzzle voltage is overlaid and shows: 1) high rail voltage until commutation occurs; 2) low current hybrid; 3) rising hybrid mode voltage; 4) plasma mode voltage; and 5) an increase at launch. 5B is a composite of the integrated rail B-dot probe data normalized by the total input current. 5C is composed from the times at which 20, 40, 60 and 80% of the input current was recorded at each of the eight rail B-dot points along with the estimated projectile trajectory.

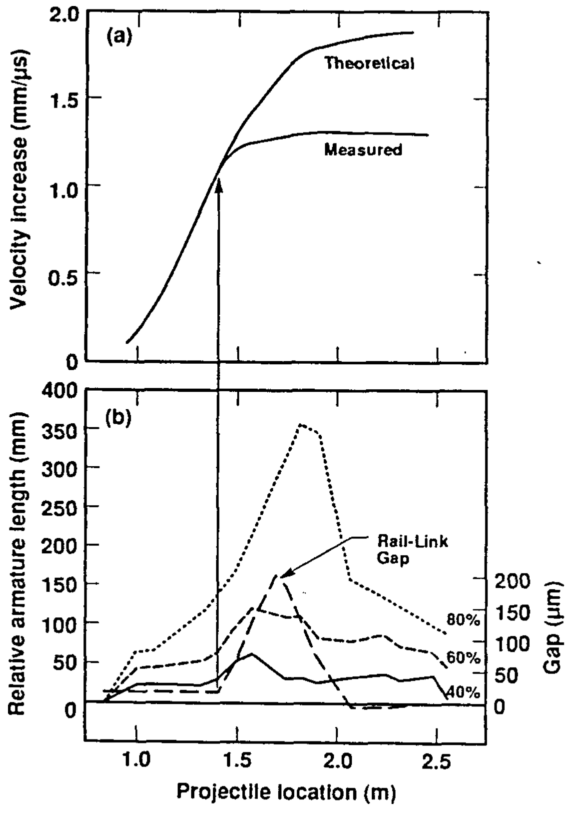

Fig. 6. Plots of extracted data vs. projectile position for H78. 6A shows the theoretical and measured velocity increase. Close agreement is achieved for about half a meter of travel resulting in a velocity increase of about 1.15 km/s followed by a divergence from the theoretical. 6B shows the relative location of the 40, 60, and 80% points relative to the 20% point as extracted from fixed time slices of the trajectories shown in Fig 5C. The minimum preshot gap between the metal armature link and rail is also shown. There is a strong correspondence between the point at which the projectile reaches the beginning of the gap increase, the point at which the gap begins to widen and the position at which performance begins to diminish. This correspondence supports the hypothesis that the vaporizing metal link is needed to replenish the plasma in order to maintain propulsion at high velocity.

DISCUSSION OF THE RESULTS

The improvement in performance obtained with the Starfire system is illustrated by H78. Fig. 7 is the deconvolved performance ratio extracted from the best of all tests performed in the early 80's with the LLNL railgun system [14]. This deconvolved relationship clearly indicates projectile acceleration diminishes to zero as the velocity approaches 7 km/s. The curve fit is described by:

$$\xi = 101 + 11.5v - 3.97\, v^2 \qquad \text{(Eq. 2)}$$

for $v \geq 3$ km/s where ξ is in percent and v is in km/s. The results obtained in H78 for the high performance portion of the acceleration from 5.5 to 6.6 km/s in the first half meter of the railgun is also shown in Fig. 7. A major improvement is clearly evident. Means to reduce the rate of plasma loss and maintain a compact and propulsive armature are under development.

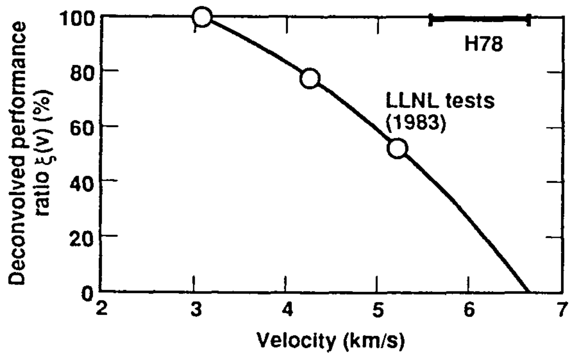

Fig. 7. Deconvolved performance ratio vs. velocity. The curve shown was found to provide a match to all the best test results from a series performed at LLNL in the early '80's [14]. The high performance of H78 for the first half meter of acceleration (up to the point at which the metal link to rail gap started to increase) is also shown. The performance ratio of H78 is much better than that obtained in the 1983 LLNL test F6 where ξ had dropped from ~40% to < 5% while the projectile accelerated from 5.6 to 6.6 km/s.

CONCLUSIONS

There are too major conclusions to be drawn from the work reported here. First, the HELEOS system has successfully demonstrated the feasibility of using a 2SLGG as a hypervelocity injector for a railgun. This has resulted in successfully performing hypervelocity railgun tests without accumulated ablation products nor restrike in a velocity regime that heretofore has suffered enormous performance losses [14, 15, 16]. Second, high performance at high velocity has been achieved. In the tests reported here, we have recorded an overall test performance ratio of 75%. Furthermore we observed nearly 100% performance throughout a railgun velocity increase of about 1.1 km/s in a velocity range that previously experienced rapid loss of performance. This is at least a crack and perhaps a breakthrough in the "performance" barrier [17]. We attribute this success to the use of the 2SLGG injector and a new projectile concept which appears to be extendable to significantly higher velocities and/or larger and more massive projectiles.

ACKNOWLEDGEMENTS

The support and encouragement of J. Chase, S. Cochran, D. Hayes and W. Herrmann have been instrumental in the execution of this project. The authors are pleased to acknowledge B. Clancy for his valuable contributions to the project and C. Sanchez for preparing this manuscript.

REFERENCES

[1] R. S. Hawke, A. R. Susoeff, J. R. Asay, J. K. Balk, C. A. Hall, C. H. Konrad, M. J. McDonald, K. W. Schuler, G. W. Wellman, R. J. Hickman, M. Shahipoor and J. L. Sauve', "STARFIRE: Hypervelocity Railgun Development for High Pressure Research," *IEEE Trans. Mag.*, Mag-25(1) 223-227 (1989).

[2] R. S. Hawke, "Railgun Development for EOS Applications: A Status Report," *Shock Waves in Condensed Matter*, S. C. Schmidt and N. C. Holmes, Eds. (North Holland, Amsterdam, 1988), pp. 643-648.

[3] M. Shahinpoor, J. R. Asay,, C. H. Konrad and C. A. Hall, "Use of a Two-Stage Light-Gas Gun as an Injector for Hypervelocity Railguns," *IEEE Trans. Mag.*, MAG-25(1), 514-518, (1989).

[4] A. C. Buckingham, "Electromagnetic Propulsion: Drag and Erosion Modeling," AIAA J., 19(11), 1422-1428 (1981).

[5] S. W. Kang and R. C. McCallen, "Plasma Behavior in the Boundary-Layer near a Railgun Surface," *IEEE Trans. Mag.*, MAG 25 (1), 217-297 (1989).

[6] R. S. Hawke, A. R. Susoeff, J. R. Asay, C. A. Hall, C. H. Konrad, R. J. Hickman, and J. L. Sauve' "Plasma Armature Formation in High-Pressure, High-Velocity Hydrogen," *IEEE Trans. Mag.*, MAG-25(1), 219-227 (1989).

[7] R. S. Hawke, J. R. Asay, C. A. Hall, R. J. Hickman, C. H. Konrad, J. L. Sauve', and A. R. Susoeff, "Armature Formation in a Railgun Using a Two-Stage Light-Gas Gun Injector," *IEEE Trans. Plasma Sci.*, 17(3), 378-385 (1989).

[8] R. Crawford, D. Keefer, and A. Sedghinasab, "Railgun Hybrid Armature, Experimental Results and Performance Characteristics," *IEEE Trans. Mag.*,? (?), ? - ? (?). [This issue].

[9] F. D. Witherspoon, GT Devices, Alexandria, VA., private communication (1989).

[10] R. L. Moody and C. H. Konrad, "Magnetic Induction System for Two-Stage Gun Projectile Velocity Measurements," SAND 84-0638 Sandia National Laboratory, Albuquerque, NM 87185 (1984).

[11] J. V. Parker, "Magnetic-Probe Diagnostics for Railgun Plasma Armatures," *IEEE Trans. Plasma Sci*, 17(3), 487-500 (1989).

[12] L. M. Smith and D. R. Keefer, "Railgun Armature Plasma-Current Density from Deconvalved B-Dot Probe Signals," *IEEE Trans. Plasma Sci.*, 17(3), 501-506 (1989).

[13] D. Keefer, A. Sedghinasab and R. Crawford, "Simultaneous Inbore Rail and Insulator Spectra From A Railgun Plasma Armature," *IEEE Trans. Mag.*, ? (?), ? - ? (?). [This issue].

[14] R. S. Hawke, W. J. Nellis, G. H. Newman, J. Rego and A. R. Susoeff, "Summary of EM Launcher Experiments Performed at LLNL," *IEEE Trans. Mag.*, MAG-22(6), 1510-1515 (1986).

[15] G. A. Shvetsov, V. M. Titov, A. G. Anisimov, Yu. L. Bashkatov and I. A. Stadnichenko, "Railgun Accelerators of Macroparticules; Part II. Experimental Investigations," *Megagauss Technology and Pulse Power Applications*, C. M. Fowler, R. S. Caird, and D. J. Erickson, Eds. (Plenum Press, New York, 1987), pp. 795-801.

[16] M. M. Kondratenko, E. F. Lebedev, V. E. Ostashev, V. I. Safonov, A. V. Ul'anov, and V. E. Fortov, "Dynamic Features of Projectile Acceleration in an Arc-Driven Railgun," *Megagauss Technology and Pulse Power Applications*, C. M. Fowler, R. S. Caird, and D. J. Erickson, Eds. (Plenum Press, New York, 1987), pp. 811-817.

[17] J. V.Parker , "Why Plasma Armature Railguns Don't Work (and What Can Be Done About It)," *IEEE Trans. Mag.*, MAG-25(1), 418-424 (1989).